ATION PAGE

Form Approved
OMB No. 0704-0188

1. AGENCY USE ONLY (Leave blank)	2. REPORT DATE	3. REPORT TYPE AND DATES COVERED
	06/30/1994	Reprint

4. TITLE AND SUBTITLE
Laser Spectroscopy of GdO: Ligand Field Assignments of $4f^7(^8S)6p \leftarrow 4f^7(S)6s$ Transitions

5. FUNDING NUMBERS
61102F 2303 ES

6. AUTHOR(S)
Leonid A. Kaledin, Matthew G. Erickson,
and Michael C. Heaven

7. PERFORMING ORGANIZATION NAME(S) AND ADDRESS(ES)
Emory University
303B School of Dentistry
Atlanta, GA 30322

8. PERFORMING ORGANIZATION REPORT NUMBER
AFOSR-TR- 94 0438

9. SPONSORING/MONITORING AGENCY NAME(S) AND ADDRESS(ES)
AFOSR/NC
Building 410, Bolling AFB DC
20332-6448

10. SPONSORING/MONITORING AGENCY REPORT NUMBER
F49620-92-J-0073

11. SUPPLEMENTARY NOTES

12a. DISTRIBUTION/AVAILABILITY STATEMENT
APPROVED FOR PUBLIC RELEASE; DISTRIBUTION IS UNLIMITED.

12b. DISTRIBUTION CODE

13. ABSTRACT *(Maximum 200 words)*

Wavelength-resolved fluorescence excitation techniques have been used to record three electronic transitions of GdO at a resolution of 0.03 cm^{-1}. Previous analyses of two bands (Yu.N. Dmitriev *et al.*, *Acta Phys. Hung.* **55**, 467 (1984) and P. Carette *et al.*, *J. Mol. Spectrosc.* **124**, 243 (1987) have been extended with some corrections to the assignments of low-J lines. Improved molecular constants were obtained for the $X^9\Sigma^-$ and $a^7\Sigma^-$ states that correlate with $Gd^{2+}(4f^7(^8S)6s)O^{2-}$. A large difference between the spin-orbit coupling constants for $X^9\Sigma^-$ (λ=-0.10353 cm^{-1}) and $a^7\Sigma^-$ (λ=-0.64712 cm^{-1}) was noted. This difference was ascribed to the fact that the *X* state is almost pure $f^7(^8S)$, whereas the *a* state has partial $f^7(^6P)$ character. Analysis of the *a* state required off-diagonal matrix elements of the spin-orbit interaction, evaluated using sixth-order degenerate perturbation theory, for treatment of non-rotating molecule spin-orbit intervals. In principle, these elements are needed to describe Σ states of septet and higher multiplicity. Energy intervals reflecting the structure $Gd^{2+}(4f^7(^8S)6p)O^{2-}$ were recognized among the excited states of GdO. Overall, the results were consistent with ligand field theory models for the excited states of lanthanide oxide (LnO) molecules.

14. SUBJECT TERMS

15. NUMBER OF PAGES

16. PRICE CODE

17. SECURITY CLASSIFICATION OF REPORT	18. SECURITY CLASSIFICATION OF THIS PAGE	19. SECURITY CLASSIFICATION OF ABSTRACT	20. LIMITATION OF ABSTRACT
UNCLASSIFIED	UNCLASSIFIED	UNCLASSIFIED	

JOURNAL OF MOLECULAR SPECTROSCOPY 165, 323–333 (1994)

Laser Spectroscopy of GdO: Ligand Field Assignments of $4f^7(^8S)6p \leftarrow 4f^7(^8S)6s$ Transitions

LEONID A. KALEDIN,[1] MATTHEW G. ERICKSON, AND MICHAEL C. HEAVEN

Department of Chemistry, Emory University, Atlanta, Georgia 30322

Wavelength-resolved fluorescence excitation techniques have been used to record three electronic transitions of GdO at a resolution of 0.03 cm^{-1}. Previous analyses of two bands (Yu.N. Dmitriev *et al., Acta Phys. Hung.* **55**, 467–479 (1984) and P. Carette *et al., J. Mol. Spectrosc.* **124**, 243–271 (1987)) have been extended with some corrections to the assignments of low-J lines. Improved molecular constants were obtained for the $X^9\Sigma^-$ and $a^7\Sigma^-$ states that correlate with $Gd^{2+}(4f^7(^8S)6s)O^{2-}$. A large difference between the spin–orbit coupling constants for $X^9\Sigma^-$ ($\lambda = -0.10353$ cm^{-1}) and $a^7\Sigma^-$ ($\lambda = -0.64712$ cm^{-1}) was noted. This difference was ascribed to the fact that the X state is almost pure $f^7(^8S)$, whereas the a state has partial $f^7(^6P)$ character. Analysis of the a state required off-diagonal matrix elements of the spin–orbit interaction, evaluated using sixth-order degenerate perturbation theory, for treatment of nonrotating molecular spin–orbit intervals. In principle, these elements are needed to describe Σ states of septet and higher multiplicity. Energy intervals reflecting the structure $Gd^{2+}(4f^7(^8S)6p)O^{2-}$ were recognized among the excited states of GdO. Overall, the results were consistent with ligand field theory models for the excited states of lanthanide oxide (LnO) molecules.

INTRODUCTION

The low-lying electronic states of several diatomic lanthanide oxides (LnO) have been successfully predicted using ligand field theory (LFT). In these models the molecular electronic structures are derived from the atomic energy levels of the divalent Ln^{2+} ions. Among the lanthanides La^{2+}, Gd^{2+}, and Lu^{2+} are distinguished by the fact that they possess $4f$ shells that are empty, half-filled, and filled, respectively. As compared to other LnO molecules, LaO and LuO have quite simple low-lying electronic structures, owing to their $4f^N(^1S_0)$ metal-ion cores. The $4f^7(^8S)$ core of Gd^{2+} is also expected to yield a relatively simple electronic structure for GdO, which may be related to the energy level patterns for LaO and LuO (see Fig. 1).

The anticipated simplicity of GdO has encouraged several spectroscopists to study states that exhibit the highest multipicities so far encountered in diatomic molecules (*1–8*). Van Zee *et al.* (*6*) established the $X^9\Sigma^-$ symmetry for ground state GdO trapped in solid argon and neon by means of ESR spectroscopy. Electronic spectra were recorded by Dmitriev *et al.* (*7*), who used pure isotopic ^{158}GdO in order to reduce line overlaps. Seventeen rotational branches were identified in a strong band at 568 nm. This transition originated from $X^9\Sigma^-$, $v = 0$. The upper level was tentatively assigned to the $\Omega = 1$ component of a $^9\Pi$ state, based on the intensity distributions of the various branches. The first excited state, $a^7\Sigma^-$, was located 1837.6(15) cm^{-1}

[1] Permanent address: High Temperature Institute of the Russian Academy of Sciences, Izhorskaya 13/19, Moscow, 127412 Russia.

0022-2852/94 $6.00

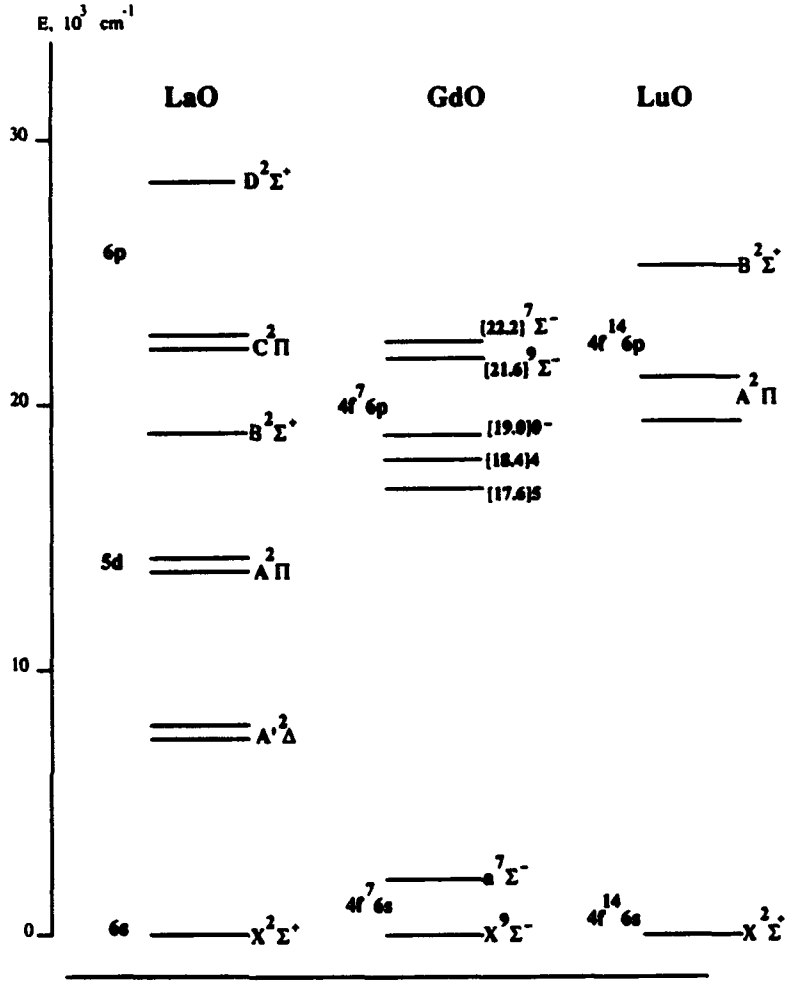

FIG. 1. Experimentally observed energy levels of LaO (*22*), GdO, and LuO (*22*).

above the $X^9\Sigma^-$ ground state. More recently, Carette *et al.* (*8*) analyzed the (0, 0) bands of the $B^9\Sigma^- - X^9\Sigma^-$ (462 nm), $B_1^7\Sigma^- - a^7\Sigma^-$ (489 nm), $B^9\Sigma^- - a^7\Sigma^-$ (504 nm), and $A^9\Pi_4 - X^9\Sigma^-$ (541 nm) transitions. In the analysis of the ground state, both Dmitriev *et al.* (*7*) and Carette *et al.* (*8*) used perturbation theory, rather than direct diagonalization of the matrix for a $^9\Sigma^-$ state.

The primary goals of the present study were to use laser spectroscopy to characterize the $X^9\Sigma^-$ and $a^7\Sigma^-$ states at 0.01 cm^{-1} accuracy, and to examine configurational assignments for excited electronic states using LFT predictions. Our measurements yield improved molecular constants for the $X^9\Sigma^-$ and $a^7\Sigma^-$ states. Spin–orbit interactions in the $a^7\Sigma^-$ state have been analyzed for the first time. We also report constants for a previously unobserved electronically excited state.

NOTATION

In the following we retain the X and a labels for the two lowest energy states. However, the alphabetical notation traditionally used to label electronically excited states becomes confusing and ambiguous when applied to the complex electronic

manifolds of systems with open d or f shells. Hence, for excited states that do not show recognizable $^{2S+1}\Lambda$ multiplet structure, we use the labels $[T_0]\Omega$, where T_0 is the term energy given in units of 10^3 cm^{-1}. For $^{2S+1}\Sigma$ states where the various Ω components are not widely separated we adopt the notation $[T_0]^{2S+1}\Sigma$. Our labels for the states reported by Carrette *et al.* (*8*) are [18.4]4 = $A^9\Pi_4$, $[21.6]^9\Sigma^- = B^9\Sigma^-$, and $[22.2]^7\Sigma^- = B_1{}^7\Sigma^-$. As described below, we found that the state previously assigned (*7*) to $^9\Pi_1$ is actually an $\Omega = 5$ state. Here we label this state as [17.6]5.

Transitions originating from the $X^9\Sigma^-$ and $a^7\Sigma^-$ states were examined in the present study. For Ω–$^7\Sigma$ or Ω–$^9\Sigma$ transitions in the Hund's case (c)–case (b) limit, there are 21 or 27 allowed rotational branches for $\Omega \neq 0$, respectively. Each of the Σ-state spin components has P, Q, and R branches. We use a $^{\Delta N}\Delta J(J'')$ branch notation, similar to the standard $^{\Delta N}\Delta J(N'')$ labels used for Hund's case (b)–case (b) transitions (*9*).

EXPERIMENTAL DETAILS

The apparatus used for this work has been described previously (*10*). ^{156}GdO vapor was obtained by resistively heating 0.1 g of isotopically pure ^{156}Gd metal to around 2400 K in the presence of 5 Torr of Ar buffer gas. GdO originated from the oxidized surface of the sample, and from reactions of the metal vapor with residual oxygen present in the vacuum system. A continuous wave ring dye laser (Coherent 699-29), capable of continuous tuning over ranges exceeding 100 cm^{-1}, was used to obtain laser excitation spectra. Wavelength-selected fluorescence excitation spectra (WSFES) were recorded using a 0.3-m McPherson monochromator to isolate the emissions of interest. Monochromator slit widths of 7–50 μm (3–20 cm^{-1}) were used for these measurements.

RESULTS AND ANALYSIS OF THE SPECTRUM

The electronic spectrum of GdO in the gas phase is very similar to the spectrum of GdO trapped in solid neon (*11*). There are two band systems in the blue region with multiheaded structures (462 nm and 489 nm bands) and several strong bands in the 525–550, 586–620, and 635–670 nm regions. Weak bands with single heads are seen in the near infrared region (*2–5, 7, 8*).

High resolution excitation spectra for the [17.6]5–$X^9\Sigma^-$ (568 nm (*7*)), [18.4]4–$X^9\Sigma^-$ (541 nm (*8*)), and [19.0]0$^-$–$a^7\Sigma^-$ (580 nm) (0, 0) bands were recorded with Doppler-limited resolution (0.03 cm^{-1}). About 600 lines of the [17.6]5–$X^9\Sigma^-$ transition were measured and assigned. Lines from all 27 rotational branches were observed. The lines for ^{156}GdO were shifted from their ^{158}GdO counterparts by less than 0.1 cm^{-1}. Consequently, the assignments of Dmitriev *et al.* (*7*) for ^{158}GdO were used to guide our rotational analysis. Assignments and positions for the first lines of the ^{156}GdO 568 nm band are given in Table I. $\Omega = 5$ was determined for the upper state from the J' values for the first P, Q, and R lines in eighteen sub-branches. We identified a total of 17 misassignments in the analysis of Dmitriev *et al.* (*7*), all of which were for nonexisting lines with $J' < 5$. These misassignments were due to the extreme congestion in the vicinity of the band origin.

Approximately 300 lines of the [18.4]4–$X^9\Sigma^-$ transition were measured and assigned. Differences between the line positions measured in the present work and those reported by Carette *et al.* (*8*) were typically less than 0.03 cm^{-1}. We identified 17 misassignments in the previous analysis (*8*), all of which were for lines with $J' < 10$. The congestion, resulting from the presence of five Gd isotopes of significant natural abundance, is the most probable reason for these misassignments.

TABLE I

Assignments and Positions of the First Rotational Lines of the [17.6]5–$X^9\Sigma^-$ Transition (cm^{-1})

ΔN	Type	J''	$^{\Delta N}R$	J''	$^{\Delta N}Q$	J''	$^{\Delta N}P$
5	*U*	4	17609.350				
4	*V*	4	17609.239	5	17607.928		
3	*T*	4	17606.597	5	17607.411	6	17606.167
2	*S*	4	17604.660	5	17604.857	6	17605.021
1	*R*	4	17601.629	5	17602.004	6	17602.147
0	*Q*	4	-	5	-	6	-
-1	*P*	4	17593.297	5	17593.733	6	17594.116
-2	*O*	4	-	5	17588.392	6	17588.882
-3	*N*	4	-	5	-	6	17582.812
-4	*M*			5	-	6	-
-5	*L*					6	-

$^{\Delta N}\Delta J(J'')$ branch notation for the Hund's case (*c*) - case (*b*) limit.

Rotationally resolved spectra for the 580 nm band have not been reported previously. About 500 lines of this feature were measured and assigned. Ten rotational branches that terminated on *f*-parity levels of the upper state were observed. Attempts to find transitions terminating on *e*-parity levels of this upper state were unsuccessful. There was a local perturbation at $J' = 43$, where the upper state level was displaced upwards by 0.11 cm^{-1}. The presence of a remote perturber was indicated by the need to use an unusually large cubic distortion constant in order to fit the rotational energies (cf. Table III). Based on the apparent absence of *e*-parity levels, we tentatively assign the upper state of the 580 nm band as $\Omega = 0^-$. However, we cannot exclude the possibility of assignment to the *f*-component of a high multiplicity Σ state with a large λ value.

Rotational Hamiltonian for the $X^9\Sigma^-$ and $a^7\Sigma^-$ States

We chose to calculate the $X^9\Sigma^-$ and $a^7\Sigma^-$ Hamiltonian matrices using a Hund's case (a) basis set (*9*). The effective Hamiltonian contained the terms (*12*)

$$H = H_{\text{rot.}} + H_{\text{s.o.}} + H_{\text{s.r.}}, \tag{1}$$

where

$$H_{\text{rot.}} = B\mathbf{R}^2 - D\mathbf{R}^4 \tag{2}$$

$$H_{\text{s.o.}} = \tfrac{2}{3}\lambda(3S_z^2 - \mathbf{S}^2) + \tfrac{1}{12}\theta(35S_z^4 - 30\mathbf{S}^2S_z^2 + 25S_z^2 - 6\mathbf{S}^2 + 3\mathbf{S}^4) + \tfrac{1}{3}\lambda_D[3S_z^2 - \mathbf{S}^2, \mathbf{R}^2]_+ \tag{3}$$

$$H_{s.r.} = \gamma \mathbf{R}\cdot\mathbf{S} + \tfrac{1}{2}\gamma_D[\mathbf{R}^2, \mathbf{R}\cdot\mathbf{S}]_+ \quad (4)$$

and $\mathbf{R} = \mathbf{J} - \mathbf{L} - \mathbf{S}$. The symbol $[x, y]_+$ denotes the anticommutator.

Cheung *et al.* (*12*) discussed the higher-order terms from Eqs. (3) and (4) that are required for states of high multiplicity. In general, $^7\Sigma$ and $^9\Sigma$ states require three and four parameters, respectively, to completely describe their (nonrotating) spin–spin intervals. The explicit forms of the matrix elements for a $^7\Sigma$ state in a Hund's case (a) basis are given in Ref. (*13*).[2] Varberg *et al.* (*13*) used fourth-order degenerate perturbation theory to include the off-diagonal matrix elements of $H_{s.o.}$. In the process of fitting our data for the $a^7\Sigma^-$ state we found that the inclusion of still higher-order spin–orbit interaction terms was necessary. For Σ states of septet and higher multiplicity the effects of the off-diagonal matrix elements of $H_{s.o.}$ were incorporated using sixth-order degenerate perturbation theory. By application of the Stevens "operator equivalents" method (*14*) we obtained the sixth-order correction

$$\langle \Lambda S\Sigma | H^{(6)}_{s.o.} | \Lambda S\Sigma\rangle = \frac{\tau}{1260}[231\Sigma^6 - 315S(S+1)\Sigma^4 + 735\Sigma^4 + 105(S(S+1))^2\Sigma^2 - 525S(S+1)\Sigma^2 + 294\Sigma^2 - 5(S(S+1))^3 + 40(S(S+1))^2 - 60S(S+1)], \quad (5)$$

where τ is a molecular constant that corresponds to b^0_0 in the notation used for solid state materials (*15*). Hamiltonian matrix elements for a $^9\Sigma$ state, evaluated in a parity adapted case (a) basis set, are given in Table II.

Determination of Molecular Constants

Molecular constants for the $X^9\Sigma^-$, $a^7\Sigma^-$, [17.6]5, [18.4]4, and [19.0]0^- states were obtained from least-squares fits that involved numerical diagonalization of the appropriate matrices. Upper state term energies were represented by the expression

$$T(J) = T_0 + BJ(J+1) - D(J(J+1))^2. \quad (6)$$

For description of the [19.0]0^- state, the cubic distortion term $H(J(J+1))^3$ term was found to be significant. Results from the least-squares fits are given in Table III. The data were not sufficiently accurate for determination of the third-order spin–rotation terms, γ_s, for $X^9\Sigma^-$ or $a^7\Sigma^-$, and these parameters were held at zero in the fits. Similarly, centrifugal distortion of the spin–rotation interaction, represented by the parameter γ_D, was statistically insignificant for $a^7\Sigma^-$. The constant representing sixth-order spin–orbit coupling was determined for $a^7\Sigma^-$, but it was too small to be characterized for $X^9\Sigma^-$.

A complete list of the line positions (in wavenumbers) measured in this study is available from the authors on request. A few copies have been deposited in the editorial office of this journal. A list of the term energies is also available. For the latter the energy zero was taken to be the $J = 4$ ($N = 0$) level of the F_1 component of the $X^9\Sigma^-$ state. The energy center-of-gravity for $a^7\Sigma^-$ was used to define the electronic term energy for this state.

[2] An error should be noted in the $\langle 3|H|2\rangle$ element given in Table II of this reference; instead of term $-2D(2x-2)$ this term should read $-\frac{1}{2}D(2x-2)$ (not $\frac{2}{2}$). The additional diagonal elements associated with Eq. (6) of the present work should be added.

TABLE II

Hamiltonian Matrix Elements for a $^9\Sigma^-$ State

	|4>	|3>	|2>	|1>	|0>
<4|	$56/3\lambda+708-4\gamma+294\gamma_D$ $+(B+56/3\lambda_D-8\gamma_D)(x-12)$ $-D(x^2-16x+48)$	$-[8(x-12)]^{1/2}(B-\gamma/2-$ $2D(x-5)-1/2\gamma_D(x-10)$ $+35/3\lambda_D-21\gamma_D]$	$-[7(x-6)(x-12)]^{1/2}(4D+$ $2\gamma_D)$		
<3|		$14/3\lambda-1058-11\gamma+(B+$ $14/3\lambda_D-11\gamma_D)(x-2)-D(x^2$ $+26x-176)-\gamma_D(11x-90)$	$-[14(x-6)]^{1/2}[B-\gamma/2$ $-2D(x+7)-1/2\gamma_D(x+34)$ $-1/3\gamma_D-6\gamma_S]$	$-[7(x-2)(x-6)]^{1/2}(6D+$ $3\gamma_D)$	
<2|			$-16/3\lambda-550-16\gamma-156\gamma+(B-$ $16/3\lambda_D-16\gamma_D)(x-12)-D(x^2+$ $56x+264)-\gamma_D(16x+60)$	$-[18(x-2)]^{1/2}[B-\gamma/2-3\gamma_D-$ $2D(x+15)-1/2\gamma_D(x+50)-$ $25/3\lambda_D+4\gamma_S]$	$-[5x(x-2)]^{1/2}(12D+6\gamma_D)$
<1|	*Symmetric*			$-34/3\lambda+458-19\gamma-54\gamma_S+(B-$ $34/3\lambda_D-19\gamma_D)(x+18)-D(x^2+74x$ $+288\pm20x)-\gamma_D(19x-18\pm10x)$	$-[40x]^{1/2}[B-\gamma/2-$ $2D(x+19)-1/2\gamma_D(x+58)$ $-13\lambda_D+9\gamma_S]$
<0|					$-40/3\lambda+908-20\gamma+(B-$ $20\gamma_D-40/3\lambda_D)(x+20)$ $D(x^2+80x+400)-20\gamma_D x$

Note. $X=J(J+1)$. The upper and lower signs for the $<1|H|1>$ element correspond to matrices of f and e symmetry, respectively. The f levels are given by the complete 5 x 5 matrix. The e levels are described by only the upper left 4 x 4 matrix, as the $|0>$ basis functions are not involved.

This matrix was constructed using a parity adapted Hund's case (a) basis set.

DISCUSSION

Fine Structure Parameters for the States Correlating with $Gd^{2+}(4f^7(^8S)6s)O^{2-}$

The present values for the $X^9\Sigma^-$ fine structure parameters ($\lambda = -0.10353(5)\ cm^{-1}$ and $\theta = -1.24(5) \times 10^{-4}\ cm^{-1}$) are in good agreement with results of Van Zee *et al.* (*6*), who examined the ESR spectrum of GdO trapped in solid Ar. The equivalent parameters derived from the solid were $|b_F^0|/2 = 0.10390(15)$ and $|b_4^0|/5 = 8(1) \times 10^{-5}\ cm^{-1}$.

In previous studies, analytical expressions for the rotational energies of a $^9\Sigma^-$ state were used. We evaluated the accuracy of these expressions by comparing the energies they predicted with those obtained by diagonalizing the $^9\Sigma^-$ Hamiltonian matrix. For parameters in the range of those found for GdO, agreement to within $\pm 0.05\ cm^{-1}$ was obtained. Note that the signs of the $X^9\Sigma^-$ λ and γ parameters (*7*, *8*) are corrected here.

Several of the $X^9\Sigma^-$ and $a^7\Sigma^-$ state fine structure parameters are explicitly related to interactions with nearby electronic states. It is important to note a significant difference between the ligand-induced state mixings for the $X^9\Sigma^-$ and $a^7\Sigma^-$ states. In the absence of configurational mixing the nonet states of GdO must be pure $f^7(^8S)$, whereas the septet states may possess some $f^7(^6P)$ character (*16*). As a consequence,

TABLE III

Constants for ^{156}GdO Derived from Laser Excitation Spectra (cm^{-1})

	$X^9\Sigma^-$	$a^7\Sigma^-$	[17.6]5[a]	[18.4]4	[19.0][b]0$^-$	[21.6]$^9\Sigma^-$	[22.2]$^7\Sigma^-$
T	0.707[c]	z[d]	17598.748(1)	18471.833(2)	z[d]+17142.612(1)	21653(2)[e]	22263[e]
B	0.355074(7)	0.356302(10)	0.353169(7)	0.349963(6)	0.356852(11)	0.338(1)[e]	0.349(1)[e]
D 10^7	2.535(16)	2.626(29)	2.601(23)	2.6 (Fixed)	-1.198(49)		
H 10^{11}					-3.01(10)		
λ	-0.10353(5)	-0.64712(11)				0.35(5)[f]	-0.05(5)[f]
θ 10^4	-1.24(5)	9.49(16)					
τ 10^4	0 (Fixed)	-6.4(22)					
λ_D 10^7	-9.4(7)	-9.2(8)					
γ 10^3	0.100(13)	1.2764(60)				-15(1)[e]	37(6)[e]
γ_D 10^8	4.6(8)	0 (Fixed)					
γ_S	0 (Fixed)	0 (Fixed)					

Note. Error limits in parentheses are one standard deviation in units of the last digits reported.

[a] The excited states are labeled using the notation $[T_0]\Omega$, where T_0 is the term energy relative to $X^9\Sigma^-$, $v = 0$, given in units of 10^{-3} cm^{-1}.

[b] Ω assignment is tentative.

[c] The $J = 4$ level of the F_1 component of the $X^9\Sigma^-$ state was taken as the energy zero.

[d] $z = 1838.3(15)$ cm^{-1}.

[e] Ref. (*7*).

[f] Calculated by the authors using information from Ref. (*7*).

it is expected that the effects of spin-orbit interactions will be more pronounced in the $a^7\Sigma^-$ state. As can be seen in Table III, this is the observed behavior. An analogous situation occurs for the $X^9\Sigma^-$ and $a^7\Sigma^-$ states of the isoelectronic species EuF, and the $X^7\Sigma^+$ and $a^5\Sigma^+$ states of MnF. For these molecules the ground states correlate with predominantly atomic S configurations while the a states may contain P character. Relatively large spin-orbit interaction parameters have been determined for the a states of EuF ($\lambda = -0.13$ cm^{-1}) (*17*) and MnF ($\lambda = 0.4139$ cm^{-1}) (*18*), while the λ values for the ground states were very much smaller (these parameters could not be determined from the available spectra). For MnF it was also noted that the $X^7\Sigma^+$ state was well represented by a single configuration, whereas the electron and nuclear spin interaction parameters for the $a^5\Sigma^+$ state could not be accounted for using a single-configuration model (*18*).

Ligand Field Theory Model for $Gd^{2+}(4f^7(^8S)6p)O^{2-}$

A LFT model for the excited states of GdO was previously developed by Carrette *et al.* (*8*). Unfortunately, this model relied heavily on an energy interval involving the formerly misassigned [17.6]5 state. We have, therefore, performed new LFT calculations that take into account the revised assignment.

Atomic selection rules indicate that metal-centered $4f^7(^8S)6p \leftarrow 4f^7(^8S)6s$ transitions should be prominent in the GdO spectrum. LFT calculation (*8*) predicts that the centers of gravity for the $4f^7(^8S)6p$ and $4f^7(^8S)6s$ configurations will be separated by roughly 18 000 cm^{-1}, giving rise to a family of transitions that span most of the visible spectral region. Hence we used a semiempirical LFT model to explore the possibility of assigning some of the excited states to the $4f^7(^8S)6p$ configuration. To begin with, it is helpful to note that this configuration gives rise to a single $\Omega = 5$ state (formally $^9\Pi_5$). It is highly probable that the [17.6]5–X transition, which is the strongest feature in the visible absorption spectrum, terminates on the unique $\Omega = 5$ state. With this assignment we found that the LFT parameters (cm^{-1}) $G(4f, 6p) = 82$ (*19*), $\zeta(6p) = 3050$ (*19*), $(\sigma - \pi)_{6p} = 4100$, and $\Delta B_0^0(6s/6p) = 18\,000$ predicted a pattern of energy levels (see Table IV) that was consistent with the positions of the known states. This pattern is most easily described by considering the effect of the ligand field on the $6p$ electron. Roughly speaking, the electric field shifts both the $6p(^2P_{3/2})$ and $6p(^2P_{1/2})$ states, and splits the former into $\Omega_{6p} = \pm\frac{1}{2}$ and $\Omega_{6p} = \pm\frac{3}{2}$ components. These effects are illustrated in Fig. 2, which shows the correlation between the $Gd^{2+}(4f^7(^8S)6p)$ free-ion and the $Gd^{2+}(4f^7(^8S)6p)O^{2-}$ states. Coupling between the $4f^7(^8S)$ core and the $6p$ electron is weak, and states belonging to a particular $|\Omega_{6p}|$ component are readily identified. Furthermore, inspection of the eigenvectors shows that $|\Lambda_{6p}|$ is a reasonably good quantum number. All of the states correlating with $6p\,(^2P_{3/2})|\Omega_{6p}| = \frac{1}{2}$ have $\Lambda_{6p} = 0$, and they correspond to $^9\Sigma^-$ and $^7\Sigma^-$ states. Here we tentatively assign the $[21.6]^9\Sigma^-$ and $[22.2]^7\Sigma^-$ states reported by Dmitriev *et al.* (*7*) and Carrette *et al.* (*8*) to the $6p(^2P_{3/2})|\Omega_{6p}| = \frac{1}{2}$ configuration. The remaining

TABLE IV

Calculated Energies (cm^{-1}) for the $4f^7(^8S)6p$ Configuration States of GdO

	Ω					
i[a]	5	4	3	2	1	0
1	17598	15180	13954	14081	14209	14295*f*
2		17956	14941	14740	14570	14471*e*
3		21152	18253	18514	18753	18950*f*
4			21100	19382	19186	19003*e*
5			22729	21067	21049	21043*f*
6				22758	22776	22781*e*

[a] Running index of states which have the same Ω values, in increasing order of energy.

Gd^{2+} free-ion parameters (*19*):

$$G(4f, 6p) = 82\ cm^{-1};\quad \zeta(6p) = 3050\ cm^{-1}.$$

Ligand field parameters:

$$(\sigma - \pi)_{6p} = 4100\ cm^{-1};\quad \text{value corresponding to } B_0^2(6p, 6p) = 6833\ cm^{-1}.$$

For definition of the $B_0^k(nl, n'l')$ parameters see Ref. (*20*).

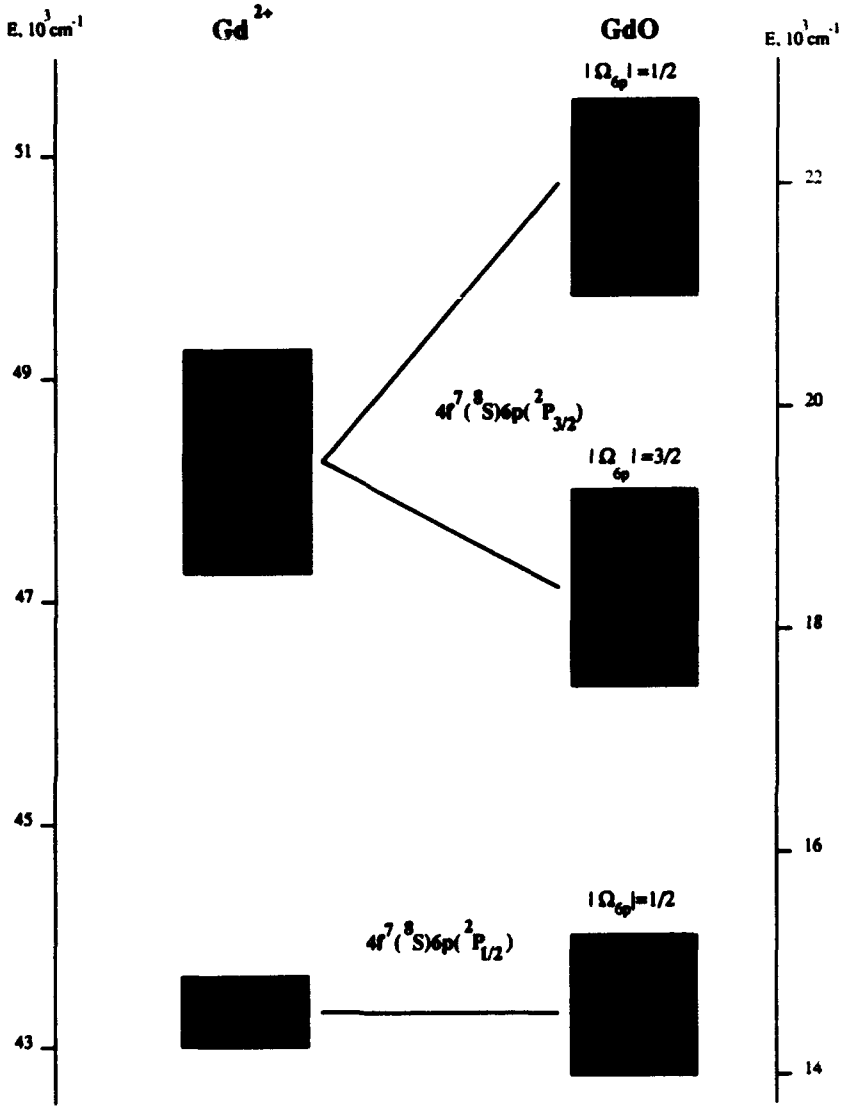

FIG. 2. Correlation between the $Gd^{2+}(4f^7(^8S)6p)$ free-ion (*23*) and the $Gd^{2+}(4f^7(^8S)6p)O^{2-}$ states (see Table IV).

states arising from $4f^7(^8S)6p(^2P)$ are formally components of the $^9\Pi$ and $^7\Pi$ multiplets; they correlate with the $6p(^2P_{3/2})|\Omega_{6p}| = \frac{3}{2}$ and $6p(^2P_{1/2})|\Omega_{6p}| = \frac{1}{2}$ configurations (the multiplicities and configurations are not correlated). Note that the separations between the $6p(^2P_{3/2})|\Omega_{6p}| = \frac{1}{2}$ and $6p(^2P_{3/2})|\Omega_{6p}| = \frac{3}{2}$ states are primarily governed by the $(\sigma - \pi)_{6p}$ "Stark splitting" term. Based on the $(\sigma - \pi)_{6p}$ values for other LnO molecules (cf. Table V), this parameter was estimated to be around 4100 cm^{-1}. From the data in Table III it is evident that the excited states examined in the present work lie approximately 4000 cm^{-1} below the $[21.6]^9\Sigma^-$ and $[22.2]^7\Sigma^-$ states. The LFT model reproduces these separations when the canonical value for $(\sigma - \pi)_{6p}$ is assumed. Thus, we tentatively assign the [17.6]5, [18.4]4, and [19.0]0^- states to the $6p(^2P_{3/2})|\Omega_{6p}| = \frac{3}{2}$ configuration. Note that the LFT calculation supports the

TABLE V

LFT Parameters for the $4f^{N+1}6p$ States of *Ln*O Molecules (cm^{-1})

LnO	Configuration lower	Configuration upper	$\Delta B_0^0(6s/6p)$[a]	Upper state $(\sigma\text{-}\pi)^b_{6p}$	Upper state $\Delta G_{1/2}$	Ref.
LaO	$6s$	$6p$	6300	4100	795	(*10*)
CeO	$4f6s$	$4f6p$	10800	4100	786	(*10*)
GdO	$4f^7(^8S)6s$	$4f^7(^8S)6p$	18000	4100		t.w.[c]
TbO	$4f^8(^7F)6s$	$4f^8(^7F)6p$	18000	4100	779	(*20*)
LuO	$4f^{14}6s$	$4f^{14}6p$	20900	3500	786	(*21*)

[a] Accuracy for these values is estimated to be ± 2000 cm^{-1}. $\Delta B_0^0(6s/6p) = B_0^0(6s/6s) - B_0^0(6p/6p)$.

[b] Stark splitting of the $6p$ orbital in the ligand field of O^{2-}.

[c] This work.

proposed Ω assignment for the $[19.0]0^-$ state, and the $6s/6p$ stabilization energy ($\Delta B_0^0(6s/6p)$) derived from the data for GdO is in good accord with the stabilization energies for other *Ln*O molecules. Table V lists the relevant LFT parameters for comparison.

SUMMARY

Improved molecular constants have been obtained for states correlating with $Gd^{2+}(4f^7(^8S)6s)O^{2-}$. A large difference between the λ values for the $X^9\Sigma^-$ and $a^7\Sigma^-$ states was noted. This was probably due to the fact that nonet states are almost pure $f^7(^8S)$, whereas the septet states can have some $f^7(^6P)$ character. High-order spin–orbit interaction terms were needed to describe the rotational levels of the $a^7\Sigma^-$ state. Additional expressions for the off-diagonal matrix elements of the spin–orbit operator, which are potentially significant for Σ states of septet or higher multiplicity, were derived using sixth-order degenerate perturbation theory.

A ligand field theory model for states arising from the $Gd^{2+}(4f^7(^8S)6p)O^{2-}$ configuration was investigated. On the basis of the model, five excited state assignments were proposed. We emphasize that these $Gd^{2+}(4f^7(^8S)6p)O^{2-}$ configurational assignments are provisional. They should be further investigated through measurements of vibrational intervals and Lande g values.

ACKNOWLEDGMENTS

We thank Professor Myron Kaufman for the use of the ring dye laser system. This work was performed under subcontract to Mission Research Corporation under contract F19628-90-C-0025 with the Phillips Laboratory, and was sponsored by the Defense Nuclear Agency (MIPR 92-586, Work Unit 00002).

RECEIVED: December 7, 1993

REFERENCES

1. J. M. EDER AND E. VALENTA, "Atlas Typischer Spectren," Springer, Vienna, 1911.
2. G. PICCARDI, *Nature* **132**, 481 and 714 (1933); *Gazz. Chim. Ital.* **63**, 887–898 (1933); *Atti Accad. Naz. Lincei. Rend.* **25**, 44–46 (1937).

3. A. GATTERER, J. JUNKES, AND E. W. SALPETER, "Molecular Spectra of Metallic Oxides." Specola Vaticana, Vatican City, 1957.
4. C. B. SUAREZ AND R. GRINFELD, *J. Chem. Phys.* **53**, 1110–1117 (1970).
5. B. R. YADAV, S. B. RAI, AND D. K. RAI, *J. Mol. Spectrosc.* **89**, 1–14 (1981).
6. R. J. VAN ZEE, R. F. FERRANTE, K. J. ZERINGUE, AND W. WELTNER, JR., *J. Chem. Phys.* **75**, 5297–5299 (1981).
7. YU. N. DMITRIEV, L. A. KALEDIN, E. A. SHENYAVSKAYA, AND L. V. GURVICH, *Acta Phys. Hung.* **55**, 467–479 (1984); YU. N. DMITRIEV, L. A. KALEDIN, A. I. KOBYLIANSKY, A. N. KULIKOV, E. A. SHENYAVSKAYA, AND L. V. GURVICH, *Acta Phys. Hung.* **61**, 51–54 (1987); L. V. GURVICH, YU. N. DMITRIEV, L. A. KALEDIN, A. I. KOBYLIANSKY, A. N. KULIKOV, AND E. A. SHENYAVSKAYA, *Bul. Acad. Sci. USSR Phys. Ser.* **48**, 93–98 (1984); **53**, 75–79 (1989).
8. P. CARETTE, A. HOCQUET, M. DOUAY, AND B. PINCHEMEL, *J. Mol. Spectrosc.* **124**, 243–271 (1987).
9. G. HERZBERG, "Spectra of Diatomic Molecules," 2nd ed., Van Nostrand, Princeton, NJ 1950.
10. L. A. KALEDIN, J. E. MCCORD, AND M. C. HEAVEN, *J. Mol. Spectrosc.* **158**, 40–61 (1993).
11. R. L. DEKOCK AND W. WELTNER, JR., *J. Phys. Chem.* **75**, 514–525 (1971).
12. A. S-C. CHEUNG, W. ZYRNICKI, AND A. J. MERER, *J. Mol. Spectrosc.* **104**, 315–336 (1984).
13. T. D. VARBERG, J. A. GRAY, R. W. FIELD, AND A. J. MERER, *J. Mol. Spectrosc.* **156**, 296–318 (1992).
14. K. W. H. STEVENS, *Proc. Phys. Soc. London Sect. A* **65**, 209–215 (1952); M. T. HUTCHINGS, *in* "Solid State Physics," (F. Seitz and D. Turnbull, Eds.), Vol. 16, pp. 227–273, Academic Press, New York, 1964.
15. W. WELTNER, JR., "Magnetic Atoms and Molecules," Van Nostrand–Reinhold, New York, 1983.
16. R. W. FIELD, private communication.
17. YU. N. DMITRIEV, L. A. KALEDIN, A. I. KOBYLIANSKY, A. N. KULIKOV, E. A. SHENYAVSKAYA, AND L. V. GURVICH, unpublished results.
18. O. LAUNILA AND B. SIMARD, *J. Mol. Spectrosc.* **154**, 93–118 and 407–416 (1992); O. LAUNILA, B. SIMARD, AND A. M. JAMES, *J. Mol. Spectrosc.* **159**, 161–174 (1993).
19. W. R. CALLAHAN, *J. Opt. Soc. Am.* **53**, 695–700 (1963).
20. R. W. FIELD, *Ber. Bunsenges. Phys. Chem.* **86**, 771–779 (1982).
21. A. N. KULIKOV, L. A. KALEDIN, A. I. KOBYLIANSKY, AND L. V. GURVICH, *Can. J. Phys.* **62**, 1855–1870 (1984).
22. K. P. HUBER AND G. HERZBERG, "Molecular Spectra and Molecular Structure. IV. Constants of Diatomic Molecules," Van Nostrand–Reinhold, Princeton, NJ 1978.
23. W. C. MARTIN, R. ZALUBAS, AND L. HAGAN, "Atomic Energy Levels—The Rare Earth Elements," NSRDS-NBS-60, 1978.